



Published in final edited form as:

Am J Med Genet A. 2015 December ; 167(12): 2957–2965. doi:10.1002/ajmg.a.37274.

***PDZD7* and hearing loss: more than just a modifier**

Kevin T Booth^{1,*}, Hela Azaiez^{1,*}, Kimia Kahrizi^{2,*}, Allen C Simpson¹, William TA Tollefson³, Christina M Sloan¹, Nicole C Meyer¹, Mojgan Babanejad², Fariba Ardalani², Sanaz Arzhang², Michael J Schnieders³, Hossein Najmabadi^{2,#}, and Richard JH Smith^{1,#}

¹Molecular Otolaryngology and Renal Research Laboratories, Department of Otolaryngology - Head & Neck Surgery, University of Iowa, Iowa City, Iowa, 52242, USA

²Genetics Research Center, University of Social Welfare and Rehabilitation Sciences, Tehran, Iran

³Department of Biomedical Engineering, University of Iowa, Iowa City, IA 52242, USA

Abstract

Deafness is the most frequent sensory disorder. With over 90 genes and 110 loci causally implicated in non-syndromic hearing loss, it is phenotypically and genetically heterogeneous. Here we investigate the genetic etiology of deafness in four families of Iranian origin segregating autosomal recessive non-syndromic hearing loss (ARNSHL). We used a combination of linkage analysis, homozygosity mapping and a targeted genomic enrichment platform to simultaneously screen 90 known deafness-causing genes for pathogenic variants. Variant segregation was confirmed by Sanger sequencing. Linkage analysis and homozygosity mapping showed segregation with the *DFNB57* locus on chromosome 10 in two families. Targeted genomic enrichment with massively parallel sequencing identified causal variants in *PDZD7*: a homozygous missense variant (p.Gly103Arg) in one family and compound heterozygosity for missense (p.Met285Arg) and nonsense (p.Tyr500Ter) variants in the second family. Screening of two additional families identified two more variants: (p.Gly228Arg) and (p.Gln526Ter). Variant segregation with the hearing loss phenotype was confirmed in all families by Sanger sequencing. The missense variants are predicted to be deleterious, and the two nonsense mutations produce null alleles. This report is the first to show that mutations in *PDZD7* cause ARNSHL, a finding that offers additional insight into the USH2 interactome. We also describe a novel likely disease-causing mutation in *CIB2* and illustrate the complexity associated with gene identification in diseases that exhibit large genetic and phenotypic heterogeneity.

Keywords

Non-syndromic hearing loss; *PDZD7*; Usher Syndrome; *DFNB57*; Modifier; Deafness

Corresponding Author: Richard J.H. Smith, 200 Hawkins Drive - 21151 PFP, The University of Iowa, Iowa City, IA 52242, Tel: +319 356 3612; Fax: +319 356 4108, richard-smith@uiowa.edu.

*co-first authors

#co-senior authors

CONFLICT OF INTEREST

The authors declare no conflict of interest.

INTRODUCTION

Many molecular factors are essential for the development and lifelong maintenance of the auditory and visual systems. Although these systems differ greatly in their anatomy and physiological processes, they share multiple molecular components. Defects in these shared proteins may impair hearing and vision.

The most common dual sensorineural disorder – Usher syndrome (USH) – is characterized by hearing loss and visual impairment. A spectrum of clinical severity exists and accordingly USH is classified into three types (USH1, USH2 and USH3) based on the degree of hearing loss, onset of retinitis pigmentosa (RP) and presence of vestibular dysfunction [Ahmed et al., 2013; Fettiplace and Kim 2014; Millan et al., 2011]. Consistent with this phenotypic variability, 10 genes have been causally implicated in USH (<http://hereditaryhearingloss.org/>). The encoded proteins participate in dynamic complexes essential for functional normality of cochlear hair cells and retinal photoreceptors.

The interactions amongst USH proteins are broadly grouped into the USH1 and USH2 interactomes. Investigating these protein networks is a highly active area of research [Avraham 2013; Blackburn et al., 2014; Lentz et al., 2013; Nagel-Wolfrum et al., 2014; Overlack et al., 2012]. In the hair cell of the inner ear, the USH2 interactome is found at the base of the stereocilia. Four proteins are vital for its formation – USH2A (OMIM 608400), VLGR1 (OMIM 602851), WHRN (OMIM 607928) and PDZD7 (OMIM 612971, NM_001195263.1). The first three are well described proteins, defects in which cause either moderate hearing loss with late onset RP and normal vestibular function (USH2), non-syndromic hearing loss (NSHL) or non-syndromic RP [Adato et al., 2005; McGee et al., 2010; Sadeghi et al., 2013; Sandberg et al., 2008]. To date, mutations in the fourth protein, PDZD7, have not been implicated alone as a cause of either USH or NSHL, however they have been shown to contribute to a digenic form of USH2 and can modify the USH2 phenotype by decreasing the age of onset and increasing the severity of RP [Ebermann et al., 2010].

PDZD7 is a scaffolding protein highly expressed in the stereocilia of inner ear hair cells [Liu et al., 2014] and in the connecting cilia of photoreceptors. It interacts via PDZ-domain binding with WHRN, USH2A and VLGR1, and in mice, it is essential for normal hearing and proper function, development and morphology of stereocilia [Chen et al., 2014; Hu et al., 2014; Zou et al., 2014]. In a zebrafish model, knockdown of *Pdzd7* results in a phenotype similar to knockdown of the other three members of the USH2 interactome [Ebermann et al., 2010]. In humans, variants in PDZD7 have been described solely as modifiers of the retinal phenotype in USH2 [Ebermann et al., 2010]. Here, we demonstrate that PDZD7 represents more than just a modifier as we directly implicate it in the physiopathology of autosomal recessive non-syndromic hearing loss (ARNSHL) in four Iranian families segregating this phenotype.

MATERIALS AND METHODS

Subjects

Four Iranian families (L-455, L-775, L-8900092 and L-8600482) segregating apparent ARNSHL were ascertained for this study. Clinical examination of the subjects was performed by an otolaryngologist, ophthalmologist and clinical geneticist. Pure tone audiometry was performed to determine air conduction thresholds at 0.25, 0.5, 1, 2, 3, 4 and 8 kHz. Ophthalmological examination was completed in all affected persons in each family. After obtaining written informed consent to participate in this study, blood samples were obtained from all family members. All procedures were approved by the human research Institutional Review Boards at the Welfare Science and Rehabilitation University and the Iran University of Medical Sciences, Tehran, Iran, and the University of Iowa, Iowa City, Iowa, USA.

Homozygosity Mapping and Haplotype Segregation Analysis

Genome-wide scan was completed in two families, L-455 and L-775, using short tandem repeat (STR) microsatellite markers as previously described [Babanejad et al., 2012; Jaworek et al., 2013]. Genotypes were resolved on an ABI 3730s Sequencer (Perkin Elmer, Waltham, MA) and analyzed using GeneMapper Software (Life Technologies, Madison, WI). Additional STRs were used to refine the *DFNB57* locus. Haplotypes were constructed manually and segregation with the deafness phenotype was confirmed in all families.

Targeted Genomic Enrichment, Massively Parallel Sequencing and Data Analysis

Targeted genomic enrichment with massively parallel sequencing (TGE+MPS) using the OtoSCOPE[®] v5 platform was performed to screen all genes implicated in NSHL and USH (90 genes; Supplemental Table I) for possible mutations in one affected person from each family [Shearer et al., 2010]. Enriched libraries were sequenced on the Illumina HiSeq 2000 (Illumina, Inc., San Diego, CA) using 100bp paired-end reads. Data analysis was performed on a local installation of the open-source Galaxy software running on a high-performance computing cluster at the University of Iowa, as described [Azaiez et al., 2014; Azaiez et al., 2015; Shearer et al., 2010]. Briefly, sequence reads were aligned using the Burrows-Wheeler Alignment (BWA) to the reference genome (hg19, NCBI Build 37). ANNOVAR and a custom workflow for variant annotation were used to annotate variants. Variants were filtered by quality (QD>10); minor allele frequency (MAF) <1% in the 1000 Genomes Project database, the National Heart, Lung, and Blood Institute (NHLBI) Exome Sequencing Project Exome Variant Server (EVS) and the Exome Aggregation Consortium (ExAC); function (exonic and splice-site); conservation (GERP and PhyloP); and pathogenicity (Polyphen2, MutationTaster, LRT and SIFT) assuming an autosomal recessive mode of inheritance. Samples were also analyzed for copy number variations (CNVs) using a sliding-window method to assess read-depth ratios [Shearer et al., 2014]. Validation and segregation of candidate variants was completed by Sanger sequencing on an ABI 3730 Sequencer (Perkin Elmer, Waltham, MA). All sequencing chromatograms were compared to published cDNA sequence; nucleotide changes were detected using Sequencher v5 (Gene Code Corporation, Ann Arbor, MI).

Molecular Modeling

Homology models for PDZ1 and PDZ2 domains in the PDZD7 protein were acquired and refined using the AMOEBA polarizable force field as a part of the Force Field X (FFX) software package [Ren et al., 2011; Shi et al., 2013]. The model refinement consisted of local minimization followed by rotamer optimization around the mutation and then a second minimization step. The first minimization step eliminates obvious steric clashes in the protein; rotamer optimization allows side chain atoms of residues near the mutation to be altered into a specific set of discrete conformations (rotamers) with low energy [Shapovalov and Dunbrack 2011]; and the final minimization step allows rigid conformations in side chains to relax. The original model was first refined using this protocol to remove model bias before modeling mutations; wild-type and mutant models were superimposed using the PyMOL molecular visualization program.

RESULTS

Subjects

Ascertained families originated from different parts of Iran: North East (L-445 and L-8900092), Central (L-755) and North West (L-8600482) (Table I). Families L-8900092, L-8600482 and L-445 reported consanguinity (Figure 1A, C–D). Physical examination in affected persons was remarkable only for hearing loss. Audiological examination in affected individuals in families L-445 and L-755 revealed prelingual mild-moderate downsloping to severe hearing loss in high frequencies whereas the two patients in family L-8900092 reported prelingual severe-profound hearing loss across all frequencies (Figure 1A–B and D). In family L-8600482 two different phenotypes were observed. The proband (II.2) presented with severe-to-profound hearing loss whereas the sibling (II.1) has mild-moderate downsloping to severe hearing loss in high frequencies (Figure 1C) similar to the phenotypes observed in families L-445 and L-775. Ophthalmological examination revealed no abnormalities on funduscopy. In family L-445, three patients had a refractory error, myopia (–3.75), corrected with contact lens and/or glasses.

Homozygosity Mapping and Haplotype Segregation Analysis

Genome-wide scanning was completed on two families: L-445 and L-775. In family L-445 linkage analysis identified a single region of homozygosity-by-descent that segregated with the hearing loss phenotype. The region mapped to chr10q21.2–q26.13 between markers D10S1652 and D10S587 (60 Mb) with a maximum LOD score of 3.26. This interval was further refined to 34Mb between markers D10S1686 and D10S1693, an interval that overlaps with the reported deafness locus, *DFNB57* (10q23.1–q26.11) (Figure 1A). In Family L-775, affected individuals shared haplotypes between markers D10S185 and D10S597 (Figure 1B). Proximal and distal boundaries were defined by Individual II.3 (between markers D10S185 and D10S192) and his sister II.4 (between markers D10S192 and D10S597), respectively. *DFNB57* lies distal to a known deafness gene, *CDH23*, and proximal to a candidate deafness gene, *TECTB*. Direct sequencing of both of these genes was normal.

Variant Identification

TGE+MPS on probands from each family generated an average of 6.9 million reads per person with an average coverage of 620 and greater than 99% coverage at 20X (Table II). Variant filtering applying the guidelines described in Materials and Methods yielded an average of 6 variants per sample (Table II). In three of the families, only variants in *PDZD7* (NM_001195263.1) represented plausible deafness-causing candidates because of their high conservation and pathogenicity prediction. As expected, probands from consanguineous families were homozygotes for these variants, while the proband from L-755 was a compound heterozygote. In family L-8600482, two plausible mutations were identified - one in *PDZD7* and one in *CIB2* (NM_006383). There were no other plausible deafness-causing variants. CNV analysis was negative (Table II).

PDZD7 Variant Analysis

Segregation analysis was completed for all families in all individuals for whom DNA samples were available. In family L-455, all affected persons were homozygous for a single *PDZD7* variant, c.307G>C (p.Gly103Arg), which lies in the PDZ1 domain of the protein (Figure 2A) and has a MAF of 0.007% and 0.0008% in EVS and ExAC, respectively. Two novel *PDZD7* variants were identified in family L-755: a missense mutation c.854T>G (p.Met285Arg) and a nonsense mutation c.1500C>A (p.Tyr500Ter): all affected individuals were compound heterozygotes, while the unaffected sibling carried only (p.Tyr500Ter). The (p.Met285Arg) mutation is located in the PDZ-2 domain (Figure 2A). In consanguineous families L-8900092 and L-8600482, homozygous mutations c.1576C>T (p.Gln526Ter) and c.682G>A (p.Gly228Arg; also in PDZ-2), respectively, were identified in affected probands. In Family L-8600482, a novel mutation in *CIB2* c.223G>A (p.Val75Met) was also identified in the proband but this variant did not segregate with the deafness phenotype in the family (Figure 1C). All three missense mutations in *PDZD7* and the single missense variant in *CIB2* are in conserved amino acids and predicted to be deleterious by Polyphen2, SIFT, Mutation Taster and LRT (Table III). None of these mutations was seen in 300 ethnically matched controls.

Molecular Modeling and Mutation Analysis

Two of the missense mutations involve identical amino acid changes although in different PDZ domains (p.Gly103Arg in PDZ1; p.Gly228Arg in PDZ2). For both of these mutants, the glycine residue present in the wild type structure is in a backbone conformation that is not typically seen with arginine ($\phi = 74^\circ$, $\psi = 175^\circ$ for Gly103 in PDZ1; $\phi = 80^\circ$, $\psi = 170^\circ$ for Gly228 in PDZ2). In addition to a decrease in backbone conformational flexibility, mutation from glycine to positively charged arginine results in new interactions with backbone or side chains amino acids (Figure 2B–C). The (p.Met285Arg) substitution in the PDZ2 domain replaces a polar methionine with the positively charged arginine, which results in different side chain interactions and backbone movement upstream in the sequence (Figure 2D). In all three cases, the mutations occur on the surface of a PDZ domain, which suggests a disease mechanism based on alteration of intermolecular PDZ interactions, as opposed to destabilizing the fold of the PDZ domain in isolation.

DISCUSSION

In this study, we implicate pathogenic variants in *PDZD7* as a novel cause of ARNSHL. *PDZD7* encodes a 1033 amino acid protein, PDZD7, which has three PDZ-domains and one harmonin-N-like (HNL) domain [Chen et al., 2014;Schneider et al., 2009] (Figure 2A). Expressed in the sensory cells of the inner ear and retina, PDZD7 is highly homologous to two other proteins with similar expression patterns, harmonin and whirlin, both of which are well described scaffolding proteins that give rise to USH or ARNSHL when mutated [Ebermann et al., 2010;Grati et al., 2012;Hu et al., 2014]. This shared similarity suggests that PDZD7 is also a scaffolding protein and functions as such in the ear and the eye.

In the cochlea, PDZD7 localizes to the base of stereocilia along with other USH-related proteins: USH2A, VLGR1 and WHRN [Grati et al., 2012;Zou et al., 2014]. These proteins are an indispensable part of the USH2 interactome and form the ankle links, a narrow web-like network that runs parallel to the apical surface of hair cells just above the insertion of stereocilia, connecting each stereocilium to its nearest neighbors [Ahmed et al., 2013]. USH2A and VLGR1 are large proteins with extensive and dissimilar extracellular domains that form the network described above. In common to both, however, are cytoplasmic PDZ-binding motifs (PBMs), which facilitate cytoplasmic protein-protein interactions [Millan et al., 2011]. Although initially posited that WHRN, with its three PDZ-domains, effectively coupled VLGR1 and USH2A, and in turn anchored the entire complex cytoplasmically at the base of the stereocilia, recent evidence suggests a more complex picture [Chen et al., 2014;Zou et al., 2014].

Mouse mutants homozygous for the targeted deletion of *Pdzd7* have congenital profound deafness as assessed by auditory brainstem response testing, although their electroretinogram responses from both rod and cone photoreceptors are normal at 1 month of age. At the microscopic level, stereocilia bundles are disorganized, and at the molecular level, localization of the USH2 interactome is disrupted, implying a direct role for PDZD7 in organizing the ankle links in the developing cochlea [Zou et al., 2014].

PDZD7 forms homodimers through its PDZ2 domains. These domains also interact with VLGR1 through the latter's cytoplasmic PBM, and heterodimerize with WHRN through its PDZ2 domain. While PDZD7 also has the ability to interact with USH2A, the PDZD7/USH2A interactions are weak and not preferential [Chen et al., 2014]. The functional role of the other domains of PDZD7 (PDZ1, PDZ3 and HNL) remains to be determined.

The five mutations we identified in *PDZD7* are conserved and predicted to have a deleterious impact on protein function (Table III). Of the three missense mutations, one – (p.Gly103Arg) – is in the PDZ1 domain while the remaining two – (p.Gly228Arg) and (p.Met285Arg) – are in the PDZ2 domain (Figure 2A). Interestingly, two of the missense changes are identical, changing a small polar glycine to a large bulky basic arginine, which by modeling alters the conformation of PDZ1 and PDZ2 (Figure 2B–C, Supplement Figure 1), (p.Met285Arg) has a similar effect (Figure 2D). These changes suggest that the decreased flexibility of PDZ2 impedes binding with VLGR1 and/or WHRN. The two nonsense mutations, (p.Tyr500Ter) and (p.Gln526Ter), lie outside functional domains

(Figure 2A), but are predicted to yield null alleles by nonsense-mediated mRNA decay (NMD) [Lu et al., 2009]. As such, affected persons in family L-8900092 have no functional copies of *PDZD7*; in contrast, affected L-755 family members carry both (p.Met285Arg) and (p.Tyr500Ter) and will have one fully translated allele with impaired binding to WHRN and/or VLGR1. In families L-455 and L-8600482, both copies of *PDZD7* are translated but the segregating mutations are predicted to disrupt protein interactions with their respective PDZ domains (Figure 2E). Although protein modeling is a robust prediction tool for structural impacts of missense mutations, its underlying assumption of protein production from the mutated allele may be inaccurate. Further functional studies are needed to fully assess and understand the consequences of the identified variants on gene expression and protein function and interactions.

Mutations in *PDZD7* have been described to modify the retinal phenotype of USH2 or have been implicated in digenic USH. All patients with divergent phenotypes had moderate downslowing hearing loss with either more severe or milder RP than expected, as summarized in Table III [Ebermann et al., 2010; Kim et al., 2015]. While these patients carried *USH2A* mutations, they were also heterozygous for mutations in *PDZD7*. In one patient the mutation, p.Arg56ProfsX24 was identified. This patient had a more severe retinal phenotype. In another patient, a splice mutation c.1750-2A>G was identified; this change causes an in-frame insertion that disrupts the HNL domain while probably preserving the PDZ3 domain. This patient had less severe RP. Finally, two patients have been described with mutations in *ADGRV1* and *PDZD7*. The first patient had an USH2 phenotype and one mutation in *ADGRV1*. After screening the coding sequence of all USH related genes, the authors identified a frameshift mutation in *PDZD7* (p.Cys732LeufsX18), raising the possibility that this mutation in combination with the *ADGRV1* mutation might be USH causing. The second patient had mild NSHL with one mutation in *ADGRV1* and one mutation in *PDZD7* [Kim et al., 2015]. USH2 was not excluded as the patient was too young to exhibit RP and so it remains unclear whether this case represents digenic USH or digenic NSHL. Phenotypic ambiguity of NSHL mimics versus true NSHL was also raised by Schneider and colleagues in an 8-year-old patient with a homozygous reciprocal translocation that disrupted the open reading frame of *PDZD7* [Schneider et al., 2009].

The absence of RP is noteworthy in the families we studied. This finding suggests that the functional roles of *PDZD7* in the retina are compensated for by other scaffolding proteins. With respect to the hearing loss, three of the families we report have a downslowing audiogram, which matches the audiometric profiles of other USH2 genes [Sadeghi et al., 2013; Steele-Stallard et al., 2013]. Persons in family L-8900092, however, have profound hearing loss across all frequencies that may reflect the fact that these patients segregate with a homozygous stop mutation. Family L-8600482 segregates with two different audio profiles; profound across all frequencies in one person and a mild-moderate downslowing to severe loss in the sibling. Interestingly, the person with the more severe phenotype also carries a homozygous mutation in the *CIB2* gene, mutation of which is responsible for *DFNB48* and Usher Syndrome type 1J (*USH1J*) [Riazuddin et al., 2012] (Figure 1D). This variant is novel and is predicted to be pathogenic by multiple pathogenicity prediction algorithms. It is located in the first EF-hand domain of the *CIB2* protein, between two

previously described pathogenic mutations that alter protein conformation and negatively affect calcium binding. We hypothesize that this novel variant has a similar effect [Jan 2013;Riazuddin et al., 2012]. The phenotype of this person matches the deafness phenotype associated with mutations in *CIB2*, making it possible that the *CIB2* mutation is causally related to the more severe phenotype. It is interesting that this person segregates two mutations in two USH-related genes and yet at the age of 33 years old does not have any vision problems.

In diseases that exhibit extensive genetic and phenotypic variability, such as deafness, identifying the genetic cause of disease can be difficult. With over 100 genes causally related to hearing loss (<http://hereditaryhearingloss.org>), providing an accurate interpretation of patients' results can be difficult [Rehman et al., 2014;Richards et al., 2015]. Each misdiagnosed case is a missed opportunity for clinical intervention and appropriate genetic counseling. Until now, patients segregating possibly pathogenic alleles in *PDZD7* have been left undiagnosed largely due to the restriction of *PDZD7*'s role as only a modifier of the USH2 phenotype. Here we correct this misinterpretation and expand the phenotypic spectrum related to *PDZD7*.

In summary, we have identified *PDZD7* as the gene responsible for ARNSHL at the *DFNB57* locus. Our finding adds to the phenotypic spectrum associated with mutation of *PDZD7* and offers additional insight into the USH2 interactome. We also describe a novel disease-causing mutation in *CIB2* and illustrate the complexity associated with gene identification in diseases that exhibit large genetic and phenotypic heterogeneity. Further studies aimed at clarifying the complex interactions of the USH2 interactome are needed to define what drives phenotypic differences, as this knowledge may offer novel strategies to alter expected phenotypes in subtle but clinically important ways.

Supplementary Material

Refer to Web version on PubMed Central for supplementary material.

Acknowledgments

We thank the families reported here for their collaboration in this study. This research was supported in part by NIDCD RO1s DC003544, DC002842 and DC012049 to RJHS.

REFERENCES

- Adato A, Lefevre G, Delprat B, Michel V, Michalski N, Chardenoux S, Weil D, El-Amraoui A, Petit C. Usherin, the defective protein in Usher syndrome type IIA, is likely to be a component of interstereocilia ankle links in the inner ear sensory cells. *Hum Mol Genet.* 2005; 14:3921–3932. [PubMed: 16301217]
- Ahmed ZM, Frolenkov GI, Riazuddin S. Usher proteins in inner ear structure and function. *Physiol Genomics.* 2013; 45:987–989. [PubMed: 24022220]
- Avraham KB. Rescue from hearing loss in Usher's syndrome. *N Engl J Med.* 2013; 369:1758–1760. [PubMed: 24171523]
- Azaiez H, Booth KT, Bu F, Huygen P, Shibata SB, Shearer AE, Kolbe D, Meyer N, Black-Ziegelbein EA, Smith RJ. TBC1D24 mutation causes autosomal-dominant nonsyndromic hearing loss. *Hum Mutat.* 2014; 35:819–823. [PubMed: 24729539]

- Azaiez H, Decker AR, Booth KT, Simpson AC, Shearer AE, Huygen PL, Bu F, Hildebrand MS, Ranum PT, Shibata SB, Turner A, Zhang Y, Kimberling WJ, Cornell RA, Smith RJ. HOMER2, a Stereociliary Scaffolding Protein, Is Essential for Normal Hearing in Humans and Mice. *PLoS Genet.* 2015; 11:e1005137. [PubMed: 25816005]
- Babanejad M, Fattahi Z, Bazazzadegan N, Nishimura C, Meyer N, Nikzat N, Sohrabi E, Najmabadi A, Jamali P, Habibi F, Smith RJ, Kahrizi K, Najmabadi H. A comprehensive study to determine heterogeneity of autosomal recessive nonsyndromic hearing loss in Iran. *Am J Med Genet A.* 2012; 158A:2485–2492. [PubMed: 22903915]
- Blackburn C, Buckingham M, Dejana E, De Luca M, Wood K, Watt F, Zammit P, Clementi E, Bordignon C, Rochat A, Munoz-Canoves P, Balling R, Bosio A, Dando J. Fighting blindness of Usher syndrome: diagnosis, pathogenesis, and retinal treatment (TreatRetUsher) (TREATRUSH). *Hum Gene Ther Clin Dev.* 2014; 25:70–71. [PubMed: 24933568]
- Chen Q, Zou J, Shen Z, Zhang W, Yang J. Whirlin and PDZ domain-containing 7 (PDZD7) proteins are both required to form the quaternary protein complex associated with Usher syndrome type 2. *J Biol Chem.* 2014; 289:36070–36088. [PubMed: 25406310]
- Ebermann I, Phillips JB, Liebau MC, Koenekoop RK, Schermer B, Lopez I, Schafer E, Roux AF, Dafinger C, Bernd A, Zrenner E, Claustres M, Blanco B, Nurnberg G, Nurnberg P, Ruland R, Westerfield M, Benzing T, Bolz HJ. PDZD7 is a modifier of retinal disease and a contributor to digenic Usher syndrome. *J Clin Invest.* 2010; 120:1812–1823. [PubMed: 20440071]
- Fettiplace R, Kim KX. The physiology of mechano-electrical transduction channels in hearing. *Physiol Rev.* 2014; 94:951–986. [PubMed: 24987009]
- Grati M, Shin JB, Weston MD, Green J, Bhat MA, Gillespie PG, Kachar B. Localization of PDZD7 to the stereocilia ankle-link associates this scaffolding protein with the Usher syndrome protein network. *J Neurosci.* 2012; 32:14288–14293. [PubMed: 23055499]
- Hu QX, Dong JH, Du HB, Zhang DL, Ren HZ, Ma ML, Cai Y, Zhao TC, Yin XL, Yu X, Xue T, Xu ZG, Sun JP. Constitutive Gα_q coupling activity of very large G protein-coupled receptor 1 (VLGR1) and its regulation by PDZD7 protein. *J Biol Chem.* 2014; 289:24215–24225. [PubMed: 24962568]
- Jan A. Mutations in CIB2 calcium and integrin-binding protein disrupt auditory hair cell calcium homeostasis in Usher syndrome type 1J and non-syndromic deafness DFNB48. *Clin Genet.* 2013; 83:317–318. [PubMed: 23331261]
- Jaworek TJ, Richard EM, Ivanova AA, Giese AP, Choo DI, Khan SN, Riazuddin S, Kahn RA, Riazuddin S. An alteration in ELMOD3, an Arl2 GTPase-activating protein, is associated with hearing impairment in humans. *PLoS Genet.* 2013; 9:e1003774. [PubMed: 24039609]
- Kim NK, Kim AR, Park KT, Kim SY, Kim MY, Nam JY, Woo SJ, Oh SH, Park WY, Choi BY. Whole-exome sequencing reveals diverse modes of inheritance in sporadic mild to moderate sensorineural hearing loss in a pediatric population. *Genet Med.* 2015
- Lentz JJ, Jodelka FM, Hinrich AJ, McCaffrey KE, Farris HE, Spalitta MJ, Bazan NG, Duelli DM, Rigo F, Hastings ML. Rescue of hearing and vestibular function by antisense oligonucleotides in a mouse model of human deafness. *Nat Med.* 2013; 19:345–350. [PubMed: 23380860]
- Liu H, Pecka JL, Zhang Q, Soukup GA, Beisel KW, He DZ. Characterization of transcriptomes of cochlear inner and outer hair cells. *J Neurosci.* 2014; 34:11085–11095. [PubMed: 25122905]
- Lu H, Lin L, Sato S, Xing Y, Lee CJ. Predicting functional alternative splicing by measuring RNA selection pressure from multigenome alignments. *PLoS Comput Biol.* 2009; 5:e1000608. [PubMed: 20019791]
- McGee TL, Seyedahmadi BJ, Sweeney MO, Dryja TP, Berson EL. Novel mutations in the long isoform of the USH2A gene in patients with Usher syndrome type II or non-syndromic retinitis pigmentosa. *J Med Genet.* 2010; 47:499–506. [PubMed: 20507924]
- Millan JM, Aller E, Jaijo T, Blanco-Kelly F, Gimenez-Pardo A, Ayuso C. An update on the genetics of usher syndrome. *J Ophthalmol.* 2011; 2011:417217. [PubMed: 21234346]
- Nagel-Wolfrum K, Baasov T, Wolfrum U. Therapy strategies for Usher syndrome Type 1C in the retina. *Adv Exp Med Biol.* 2014; 801:741–747. [PubMed: 24664766]

- Overlack N, Goldmann T, Wolfrum U, Nagel-Wolfrum K. Gene repair of an Usher syndrome causing mutation by zinc-finger nuclease mediated homologous recombination. *Invest Ophthalmol Vis Sci.* 2012; 53:4140–4146. [PubMed: 22661463]
- Rehman AU, Santos-Cortez RL, Drummond MC, Shahzad M, Lee K, Morell RJ, Ansar M, Jan A, Wang X, Aziz A, Riazuddin S, Smith JD, Wang GT, Ahmed ZM, Gul K, Shearer AE, Smith RJ, Shendure J, Bamshad MJ, Nickerson DA, University of Washington Center for Mendelian G. Hinnant J, Khan SN, Fisher RA, Ahmad W, Friderici KH, Riazuddin S, Friedman TB, Wilch ES, Leal SM. Challenges and solutions for gene identification in the presence of familial locus heterogeneity. *Eur J Hum Genet.* 2014
- Ren P, Wu C, Ponder JW. Polarizable Atomic Multipole-based Molecular Mechanics for Organic Molecules. *J Chem Theory Comput.* 2011; 7:3143–3161. [PubMed: 22022236]
- Riazuddin S, Belyantseva IA, Giese AP, Lee K, Indzhukulian AA, Nandamuri SP, Yousaf R, Sinha GP, Lee S, Terrell D, Hegde RS, Ali RA, Anwar S, Andrade-Elizondo PB, Sirmaci A, Parise LV, Basit S, Wali A, Ayub M, Ansar M, Ahmad W, Khan SN, Akram J, Tekin M, Riazuddin S, Cook T, Buschbeck EK, Frolenkov GI, Leal SM, Friedman TB, Ahmed ZM. Alterations of the CIB2 calcium- and integrin-binding protein cause Usher syndrome type 1J and nonsyndromic deafness DFNB48. *Nat Genet.* 2012; 44:1265–1271. [PubMed: 23023331]
- Richards S, Aziz N, Bale S, Bick D, Das S, Gastier-Foster J, Grody WW, Hegde M, Lyon E, Spector E, Voelkerding K, Rehm HL. Standards and guidelines for the interpretation of sequence variants: a joint consensus recommendation of the American College of Medical Genetics and Genomics and the Association for Molecular Pathology. *Genet Med.* 2015
- Sadeghi AM, Cohn ES, Kimberling WJ, Halvarsson G, Moller C. Expressivity of hearing loss in cases with Usher syndrome type IIA. *Int J Audiol.* 2013; 52:832–837. [PubMed: 24160897]
- Sandberg MA, Rosner B, Weigel-DiFranco C, McGee TL, Dryja TP, Berson EL. Disease course in patients with autosomal recessive retinitis pigmentosa due to the USH2A gene. *Invest Ophthalmol Vis Sci.* 2008; 49:5532–5539. [PubMed: 18641288]
- Schneider E, Marker T, Daser A, Frey-Mahn G, Beyer V, Farcas R, Schneider-Ratzke B, Kohlschmidt N, Grossmann B, Bauss K, Napiontek U, Keilmann A, Bartsch O, Zechner U, Wolfrum U, Haaf T. Homozygous disruption of PDZD7 by reciprocal translocation in a consanguineous family: a new member of the Usher syndrome protein interactome causing congenital hearing impairment. *Hum Mol Genet.* 2009; 18:655–666. [PubMed: 19028668]
- Shapovalov MV, Dunbrack RL Jr. A smoothed backbone-dependent rotamer library for proteins derived from adaptive kernel density estimates and regressions. *Structure.* 2011; 19:844–858. [PubMed: 21645855]
- Shearer AE, DeLuca AP, Hildebrand MS, Taylor KR, Gurrola J 2nd, Scherer S, Scheetz TE, Smith RJ. Comprehensive genetic testing for hereditary hearing loss using massively parallel sequencing. *Proc Natl Acad Sci U S A.* 2010; 107:21104–21109. [PubMed: 21078986]
- Shearer AE, Kolbe DL, Azaiez H, Sloan CM, Frees KL, Weaver AE, Clark ET, Nishimura CJ, Black-Ziegelbein EA, Smith RJ. Copy number variants are a common cause of non-syndromic hearing loss. *Genome Med.* 2014; 6:37. [PubMed: 24963352]
- Shi Y, Xia Z, Zhang J, Best R, Wu C, Ponder JW, Ren P. The Polarizable Atomic Multipole-based AMOEBA Force Field for Proteins. *J Chem Theory Comput.* 2013; 9:4046–4063. [PubMed: 24163642]
- Steele-Stallard HB, Le Quesne Stabej P, Lenassi E, Luxon LM, Claustres M, Roux AF, Webster AR, Bitner-Glindzicz M. Screening for duplications, deletions and a common intronic mutation detects 35% of second mutations in patients with USH2A monoallelic mutations on Sanger sequencing. *Orphanet J Rare Dis.* 2013; 8:122. [PubMed: 23924366]
- Zou J, Zheng T, Ren C, Askew C, Liu XP, Pan B, Holt JR, Wang Y, Yang J. Deletion of PDZD7 disrupts the Usher syndrome type 2 protein complex in cochlear hair cells and causes hearing loss in mice. *Hum Mol Genet.* 2014; 23:2374–2390. [PubMed: 24334608]

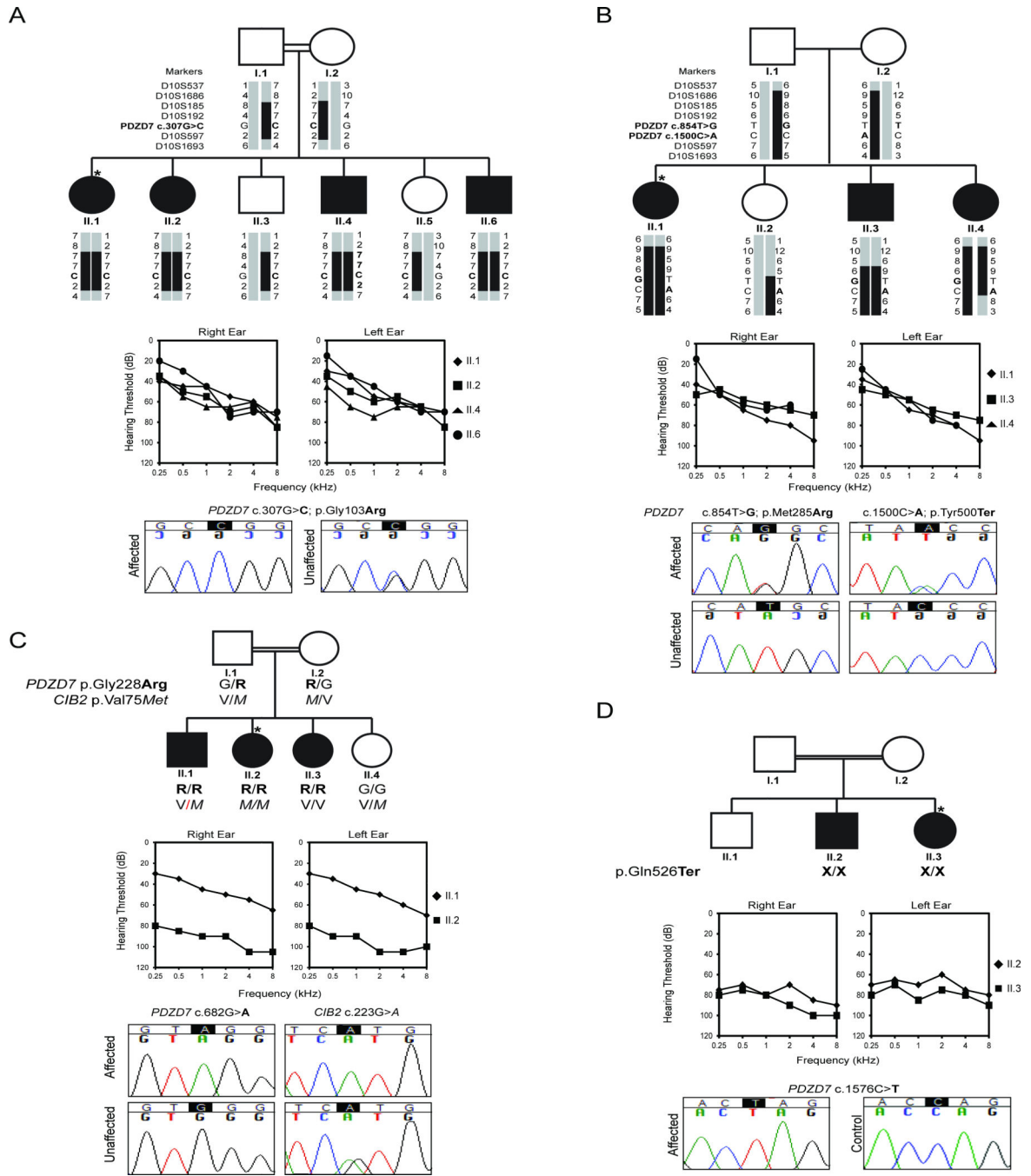


Figure 1. Pedigrees showing haplotypes in *DFNB57* locus, audiometric data and sequence chromatograms for families segregating mutations in *PDZD7*
 Males are denoted with squares and females with circles. Solid shapes are individuals with reported hearing loss. Double lines indicate consanguinity. Generation and individual identification is noted by Roman numerals. Bold denotes variant in *PDZD7* segregating with the phenotype. Italics indicate the mutation in *CIB2*. An asterisk represents the individual who underwent OtoSCOPE® testing. Audiograms were obtained using pure tone audiometry with air conduction from frequencies 250 to 8000 Hz. Sanger sequencing confirmed each mutation in the chromatogram from affected individuals and unaffected siblings or controls.

A–B) Pedigrees of families L-445 and L-755 with six haplotype markers. Solid black rectangles indicate morbid haplotype while other haplotypes are in gray. **C–D)** Pedigrees of families L-8900092 and L-8600482.

Author Manuscript

Author Manuscript

Author Manuscript

Author Manuscript

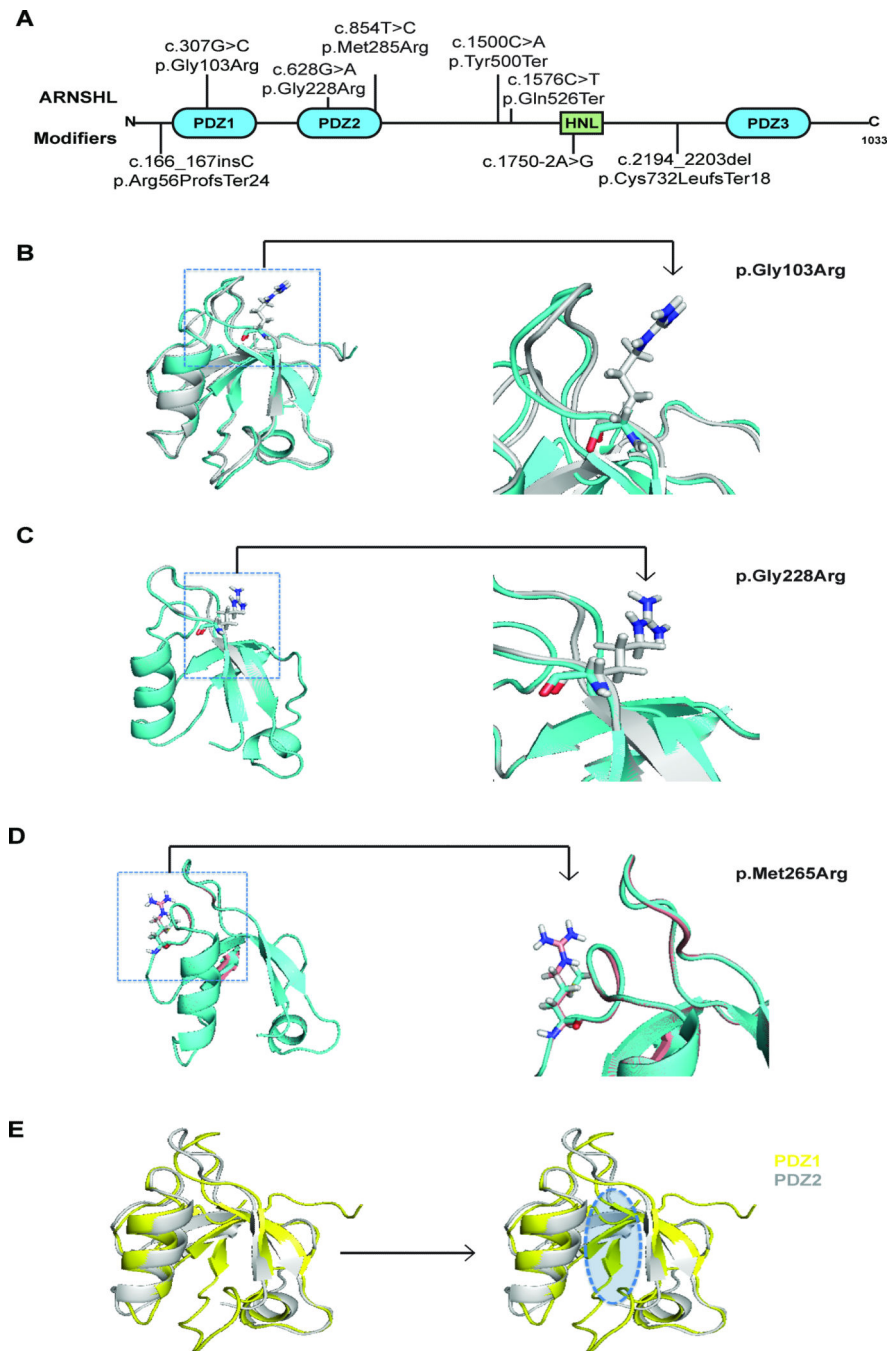


Figure 2. A schematic representation of the PDZD7 protein and structural analysis of the PDZD7 identified missense mutations

A) PDZD7 has three PDZ domains (blue) and the one harmonin-N-like domain (HNL) (green). Previously reported mutations (on bottom) modify the USH2 retinal phenotype. Shown on top are the mutations that segregate with the ARNSHL phenotype in this study. Amino acid positions are based on RefSeq NP_001182192. Domain locations are based on NCBI Conserved Domain Analysis. **B–E)** A cartoon model compares wild-type (blue) and mutated (gray) PDZ domains by superimposition. Mutated sites are highlighted by blue

circles and locally zoomed. **B)** PDZ1 domain with mutation p.Gly103Arg. **C)** PDZ2 domain with p.Gly228Arg mutation and **D)** p.Met265Arg mutation. **E)** PDZ1 (yellow) and PDZ2 (grey) structures; the blue shaded area is the binding area where a new beta sheet is formed from the c-terminus of either GPR98 or USH2A.

Author Manuscript

Author Manuscript

Author Manuscript

Author Manuscript

Table I

Clinical Summary of Patients

Family ID	L-755			L-8600482			L-445			L-8900092		
Ethnicity Region	Iranian Central-Shiraz			Iranian North East-Birjand			Iranian North West-Tabriz			Iranian North West-Tabriz		
Patient ID	II.1	II.3	II.4	II.1	II.2	II.3	II.1	II.2	II.4	II.6	II.2	II.3
Age at Examination	38	33	25	40	33	20	36	30	25	21	31	23
Ophthalmologic Examination (years)	N	N	N	N	N	N	N*	N*	N*	N	N	N
Audiologic Pattern	Down Sloping			Down Sloping/Flat			Down Sloping			Flat		
Severity of HL	Moderate-severe			Moderate-severe/Profound			Moderate-severe			Profound		
Type of HL	Prelingual			Prelingual			Prelingual			Prelingual		

N represents a normal fundoscopic report. An asterisk indicates a refractory error (myopia [-3.75]).

Table II

OtoSCOPE® Coverage Statistics

OtoSCOPE® Results										
Family ID	Patient	Average Target Coverage	Reads Overlapping Target	% Coverage			Variants after filtering	CNV	Candidate Variant(s)	
				1X	10X	20X				
L-445	II.1	622	7700415	99.88	99.59	99.35	3	0	1	
L-755	II.1	513	5976821	99.86	99.52	99.18	6	0	2	
L-8600482	II.2	648	7353056	99.93	99.68	99.44	7	0	2	
L-8900092	II.3	697	9254099	99.90	99.63	99.47	8	0	1	
Average		620	7571098	99.89	99.61	99.36	6	0	1	

Table III

PDZD7 Mutations and Phenotype Correlation

Pheno type	Family Origin	ID	Genotype	Nucleotide Change	Amino Acid Change	Domain	MAF (%)			GERP	PhyloP	Poly phen2	SIFT	Mutation Taster	LRT	Reference
							IKG	EVS	ExAC							
ARNSHL	Iranian	L-445	Homo	c.307G>C	p.Gly103Arg	PDZ1	0	.012	0.0008	C	C	D	D	D	D	This Study
		L-8600482	Homo	c.682G>A	p.Gly228Arg	PDZ2	0	0	0.0008	C	C	D	D	D	D	
		L-8900090	Homo ^a	c.94G>A	p.Val32Met	EF1	0	0	0.0008	C	C	D	D	D	D	
		L-8900090	Homo	c.1576C>T	p.Gln526Ter	-	NA	NA	0							
		L-755	Comp Het	c.854T>G c.1500C>A	p.Met285Arg p.Tyr500Ter	PDZ2	0	0	0	0	C	C	D	D	D	
USH2 Modifier	Canadian	Fac	Het	c.166_167insC	p.Arg56fsTer24	-	NA	NA	0							
			Homo ^b	c.4338_4339del	p.Cys1447fsTer	FTIII	NA	NA	0							
			Het	c.1750-2A>G	Splice Site	HNL	NA	NA	0							
		GER1	Het ^b	c.4515_4518del	p.Arg1505fsTer	-	NA	NA	0							Ebermann 2010
Hearing Loss	Korean	SB112-204	Het	c.13316C>T	p.Thr4439Ile	FTIII	0	0	0	C	C	P	T	D	U	
			Het	c.2194_2203del	p.Cys732fsTer18	-	NA	NA	0							
			Het ^c	c.17137delG	p.Ala5713fsTer	-	NA	NA	0							
	Het	c.76_77del	p.Ser26fsTer53	-	NA	NA	0							Kim 2015		
	Het ^c	c.3022+2T>G	Splice Site	-	NA	NA	0									

Nucleotide numbering: the A of the ATG translation initiation site is noted as +1 using isoform NM_001195263 of *PDZD7*, NM_006383 for *CIB2*, NM_206933 for *USH2A* and NM_032119 for *ADGRV1*. NSHL, non-syndromic hearing loss; USH2, Usher Syndrome Type 2; C, predicted Conserved; D, predicted Damaging or Deleterious; P, Probably Damaging; T, Tolerated; U, Unknown; NA, data not available; PDZ, PDZ domain; EF, EF-hand; HNL, harmonin-N-like domain; FTIII, Fibronectin type-III. Dashes denote mutations outside functional domains.

^aMutation found in *CIB2*.

^bMutations reported in *USH2A*.

^cMutations reported in *ADGRV1*.